Opt Quant Electron (2011) 42:785–791
DOI 10.1007/s11082-011-9483-6

Modified rate equation model including the photon–photon resonance

Antti Laakso · Mihail Dumitrescu

Received: 23 September 2010 / Accepted: 10 June 2011 / Published online: 23 June 2011

Abstract We show that, when the longitudinal confinement factor in an edge-emitting laser is treated as a dynamic variable, the modulation transfer function has an extra term. This term produces a supplementary photon–photon resonance peak in the modulation response at a frequency corresponding to the frequency separation between longitudinal modes, when these modes are phase-locked long enough (quasi-phase-locked). The photon–photon resonance peak is strongest when two consecutive quasi-phase-locked dominant longitudinal modes have similar longitudinal envelopes and share equally the photon population.

Keywords Longitudinal modes · Modulation response · Modulation transfer function · Photon–photon resonance · Rate equations

1 Introduction

In conventional high-speed laser devices the modulation response is largely determined by the carrier-photon resonance (CPR). However, the occurrence of the photon–photon resonance (PPR) can increase the 3-dB modulation bandwidth substantially. The PPR has been observed in distributed Bragg reflector (DBR) laser diodes (Kjebon et al. 1997; Bach et al. 2004), in coupled-cavity-injection-grating (CCIG) lasers (Kaiser et al. 2004; Gerschütz et al. 2008), and in passive-feedback lasers (Radziunas et al. 2007), but a thorough explanation for the phenomenon has not been given (Feiste 1998; Morthier et al. 2000).

A. Laakso (✉) · M. Dumitrescu
Optoelectronics Research Centre, Tampere University of Technology, P.O. Box 692, 33101 Tampere, Finland
e-mail: Antti.I.Laakso@tut.fi

2 Modified rate equations

The density rate equations can be written as:

$$\frac{dN}{dt} = \frac{\eta_i I}{qV} - \left(R_{sp} + R_{nr}\right) - v_g g N_p \tag{1}$$

$$\frac{dN_p}{dt} = \left(\Gamma v_g g - \frac{1}{\tau_p}\right) N_p + \Gamma R'_{sp} \tag{2}$$

with the same formulation and symbols as in Coldren and Corzine (1995).

The classical small-signal response is obtained by taking the differentials of (1) and (2), and considering I, N, N_p and g as dynamic variables, while $\Gamma = \Gamma_{xy}\Gamma_z$ is assumed to be time-independent (i.e. $\Gamma_z = 1$) (Coldren and Corzine 1995). When $\Gamma(z,t)$ is also treated as a dynamic variable, the differentials of (1) and (2) become:

$$d\left[\frac{dN}{dt}\right] = \frac{\eta_i}{qV} dI - \frac{1}{\tau_{\Delta N}} dN - v_g g\, dN_p - N_p v_g dg \tag{3}$$

$$d\left[\frac{dN_p}{dt}\right] = \left(\Gamma v_g g - \frac{1}{\tau_p}\right) dN_p + N_p \Gamma v_g dg + \frac{\Gamma}{\tau'_{\Delta N}} dN + \left(N_p v_g g + R'_{sp}\right) d\Gamma \tag{4}$$

where $1/\tau_{\Delta N} = dR_{sp}/dN + dR_{nr}/dN$ and $1/\tau'_{\Delta N} = dR'_{sp}/dN$. Treating $\Gamma(z,t)$ as a dynamic variable is justified because the optical field distribution in a laser cavity varies both in space and time, particularly when more than one longitudinal mode are present. The gain variation dg can be expanded to $dg = a dN - a_p dN_p$, using the differential gain terms a and a_p. As a result (3) and (4) can be written as:

$$\frac{d}{dt}\begin{bmatrix} dN \\ dN_p \end{bmatrix} = \begin{bmatrix} -\gamma_{NN} & -\gamma_{NP} \\ \gamma_{PN} & -\gamma_{PP} \end{bmatrix} \begin{bmatrix} dN \\ dN_p \end{bmatrix} + \begin{bmatrix} \frac{\eta_i}{qV} dI \\ \left(N_p v_g g + R'_{sp}\right) d\Gamma \end{bmatrix} \tag{5}$$

where γ_{NN}, γ_{NP}, γ_{PN} and γ_{PP} are rate coefficients, as defined in Coldren and Corzine (1995). To obtain the small-signal responses $dN(t)$ and $dN_p(t)$ to a current modulation $dI(t)$, we assume, as in (Coldren and Corzine 1995), the solutions:

$$dI(t) = I_1 e^{j\omega t}, \quad dN(t) = N_1 e^{j\omega t}, \quad dN_p(t) = N_{p1} e^{j\omega t} \tag{6}$$

Substituting these solutions to (5) leads to:

$$\begin{bmatrix} \gamma_{NN} + j\omega & \gamma_{NP} \\ -\gamma_{PN} & \gamma_{PP} + j\omega \end{bmatrix} \begin{bmatrix} N_1 \\ N_{p1} \end{bmatrix} = \begin{bmatrix} \frac{\eta_i I_1}{qV} \\ \left(N_p v_g g + R'_{sp}\right) \Gamma_{xy} \frac{\delta \Gamma_z(t)}{\delta t} e^{-j\omega t} dt \end{bmatrix} \tag{7}$$

The determinant of the left-hand side matrix in (7) is given by:

$$\Delta = \begin{vmatrix} \gamma_{NN} + j\omega & \gamma_{NP} \\ -\gamma_{PN} & \gamma_{PP} + j\omega \end{vmatrix} = (\gamma_{NN} + j\omega)(\gamma_{PP} + j\omega) + \gamma_{NP}\gamma_{PN} \tag{8}$$

and the resulted small-signal photon density is:

$$N_{p1} = \frac{\eta_i I_1}{qV} \frac{\gamma_{PN}}{\Delta} + \int_0^\infty \frac{(\gamma_{NN} + j\omega)(N_p v_g g + R'_{sp})\Gamma_{xy}}{\Delta} \frac{\delta \Gamma_z(t)}{\delta t} e^{-j\omega t} dt \tag{9}$$

If we neglect the time-dependence of the rate coefficients (i.e. time-averaged parameters are used in simulations) this can be further simplified to:

$$N_{p1} = \frac{\eta_i I_1}{qV}\frac{\gamma_{PN}}{\Delta} + \frac{(\gamma_{NN} + j\omega)\left(N_p \upsilon_g g + R'_{sp}\right)\Gamma_{xy}}{\Delta}\int_0^T \frac{\delta\Gamma_z(t)}{\delta t}e^{-j\omega t}dt, \quad T \to \infty \tag{10}$$

3 The modulation transfer function

When the photon field can be approximated as a sum of two dominant phase-locked longitudinal modes with frequencies ω_1 and ω_2, wave numbers k_1 and k_2, and amplitudes a_1 and a_2, the aggregated optical field intensity at position z and time t can be written as:

$$\begin{aligned}\Psi^2(z,t) &= \left|a_1(z)e^{jk_1 z}e^{-j\omega_1 t} + a_2(z)e^{jk_2 z}e^{-j\omega_2 t}\right|^2 = \left|A_1(z)e^{-j\omega_1 t} + A_2(z)e^{-j\omega_2 t}\right|^2 \\ &= |A_1(z)|^2 + |A_2(z)|^2 + A_1(z)A_2^*(z)e^{j\Delta\omega t} + A_1^*(z)A_2(z)e^{-j\Delta\omega t} \\ &= |A_1(z)|^2 + |A_2(z)|^2 + c(z)e^{j\Delta\omega t} + c^*(z)e^{-j\Delta\omega t}\end{aligned} \tag{11}$$

where $\Delta\omega = \omega_2 - \omega_1 > 0$ and $c(z) = A_1(z)A_2^*(z)$. Using (11) the integral in (10) can be written as:

$$\begin{aligned}\int_0^T \frac{\delta\Gamma_z(t)}{\delta t}e^{-j\omega t}dt &= \int_0^T \frac{\delta}{\delta t}\left(\int_0^L \Psi^2(z,t)dz\right)e^{-j\omega t}dt \\ &= j\Delta\omega\int_0^T e^{j(\Delta\omega-\omega)t}dt\int_0^L c(z)dz - j\Delta\omega\int_0^T e^{-j(\Delta\omega+\omega)t}dt\int_0^L c^*(z)dz \\ &= j\Delta\omega T e^{j(\Delta\omega-\omega)T/2}\,\mathrm{sinc}\left((\Delta\omega-\omega)T/2\right)\int_0^L c(z)dz \\ &\quad - j\Delta\omega T e^{-j(\Delta\omega+\omega)T/2}\,\mathrm{sinc}\left((\Delta\omega+\omega)T/2\right)\int_0^L c^*(z)dz \\ &= h(\omega)\end{aligned} \tag{12}$$

with $A_1(z)$ and $A_2(z)$ normalized in such a way that $\int_0^L |A_1(z) + A_2(z)|^2 dz = 1$. Accordingly, the photon density results as:

$$N_{p1} = \frac{\eta_i I_1}{qV}\frac{\gamma_{PN}}{\Delta} + \frac{(\gamma_{NN} + j\omega)\left(N_p \upsilon_g g + R'_{sp}\right)\Gamma_{xy}}{\Delta}h(\omega) \tag{13}$$

and the modulation transfer function becomes:

$$H(\omega) = \frac{\eta_i}{qV}\frac{\gamma_{PN}}{\Delta} + \frac{(\gamma_{NN} + j\omega)\left(N_p \upsilon_g g + R'_{sp}\right)\Gamma_{xy}}{I_1\Delta}h(\omega) \tag{14}$$

The first term in (14) is the traditional modulation transfer function, while the second term is associated with the PPR. Note that N_p is directly proportional to I_1 and $N_p \upsilon_g g \gg R'_{sp}$.

Consequently, contrary to what it might first seem, the second term in (14) is not inversely proportional to the modulation amplitude of the bias current. The first term in $h(\omega)$ has a maximum value at the modulation frequency $\omega = \Delta\omega$, whereas the second term in $h(\omega)$ has a maximum value at the negative modulation frequency $\omega = -\Delta\omega$. Including only the first term from $h(\omega)$ leads to a modulation transfer function given by:

$$H(\omega) = \frac{\eta_i}{qV}\frac{\gamma_{PN}}{\Delta} + \frac{(\gamma_{NN} + j\omega)\left(N_p \upsilon_g g + R'_{sp}\right)\Gamma_{xy}}{I_1 \Delta} \times j\Delta\omega T e^{j(\Delta\omega-\omega)T/2} \sin c\left((\Delta\omega - \omega)\,T/2\right) \int_0^L c(z)dz \tag{15}$$

where T is the interval for which the phase difference between the longitudinal modes is maintained.

4 Evaluation of the overlap integral

The photon–photon resonance peak gets stronger as the value of the overlap integral $\int_0^L c(z)dz$ increases. For a simple case with constant longitudinal field amplitudes, a_1 and a_2, the overlap integral is:

$$\int_0^L c(z)dz = \int_0^L a_1 e^{jk_1 z} {a_2}^* e^{-jk_2 z} dz = \frac{a_1 {a_2}^*}{j\Delta k}\left(e^{j\Delta k L} - 1\right) \tag{16}$$

where $\Delta k = k_1 - k_2$ (and $k_1 \neq k_2$). When two longitudinal modes in a Fabry-Pérot (FP) laser cavity (without a grating) are considered, Δk can be written as:

$$\Delta k = k_1 - k_2 = 2\pi\left(\frac{n_1}{\lambda_1} - \frac{n_2}{\lambda_2}\right) = \frac{\pi}{L}(m_1 - m_2) \tag{17}$$

where n_1 and n_2 are the effective refractive indices for the modes and m_1 and m_2 are integers known as mode orders. Therefore:

$$\int_0^L c(z)dz = \begin{cases} \frac{j2a_1{a_2}^* L}{\pi(m_1 - m_2)}, & \text{when } m_1 - m_2 = \pm 1,\ \pm 3,\ \pm 5,\ \ldots \\ 0, & \text{when } m_1 - m_2 = \pm 2,\ \pm 4,\ \pm 6,\ \ldots \end{cases} \tag{18}$$

When a_1 and a_2 are real numbers (which is the case when a simple cavity without a grating is considered) and $A_1(z)$ and $A_2(z)$ have been normalized as mentioned before, the following condition results:

$$a_1^2 + a_2^2 = 1/L \tag{19}$$

Furthermore, a_1 and $a_2 (a_1 \geq a_2)$ can be related to the side-mode suppression ratio (SMSR) between the two dominant longitudinal modes by:

$$\text{SMSR (dB)} = 20\log_{10}\left(\frac{a_1}{a_2}\right) \tag{20}$$

Combining Eqs. (18), (19) and (20) leads to the following approximation:

$$\int_0^L c(z)dz = \begin{cases} \frac{j}{\pi(m_1-m_2)} \frac{2\cdot 10^{\mathrm{SMSR}/20}}{1+10^{\mathrm{SMSR}/10}}, & \text{when } m_1 - m_2 = \pm 1,\ \pm 3,\ \pm 5,\ \ldots \\ 0, & \text{when } m_1 - m_2 = \pm 2,\ \pm 4,\ \pm 6,\ \ldots \end{cases} \tag{21}$$

where the SMSR is given in dB. This means that the PPR is only obtained between the longitudinal modes for which $|m_1 - m_2|$ is odd and that the PPR effect is the strongest for successive modes. The maximum value of the overlap integral is j/π, which is obtained for the successive modes when the SMSR between them is 0 dB. Under all the mentioned approximations the modulation transfer function for a laser with quasi-phase-locked successive longitudinal modes ($m_1 - m_2 = \pm 1$) becomes:

$$H(\omega) = \frac{\eta_i}{qV}\frac{\gamma_{PN}}{\Delta} + \frac{(\gamma_{NN} + j\omega)\left(N_p \upsilon_g g + R'_{sp}\right)\Gamma_{xy}}{I_1 \Delta} \times j\Delta\omega T e^{j(\Delta\omega-\omega)T/2} \sin c\left((\Delta\omega - \omega)T/2\right) \frac{j}{\pi} \frac{2\cdot 10^{\mathrm{SMSR}/20}}{1+10^{\mathrm{SMSR}/10}} \tag{22}$$

Equation (22) can be easily generalized to include several longitudinal modes.

5 Simulation results

The supplementary term in the modulation response introduces a PPR peak placed at a frequency $\Delta\lambda \cdot c/\lambda^2$, in agreement with the experimental results (Bach et al. 2004; Kaiser et al. 2004; Gerschütz et al. 2008; Radziunas et al. 2007). The PPR peak results from the fact that, when modulating at the PPR frequency, the variation of the aggregate longitudinal optical field intensity integral in the cavity is in resonance with the modulating current.

In FP lasers the separation between the CPR and PPR peaks is always high, since high-frequency CPR requires a short cavity while a close-enough PPR requires a long cavity. The simulated response, under the given assumptions, for a 1,000 μm long laser emitting at 1.3 μm and biased at 100 mA (with typical material parameters) is shown in Fig. 1. The approximation given by (21) has been used for the overlap integral and the response has been calculated for SMSR values between 10 and 60 dB. The results have been generated by simulating the modulation response at 5,000 frequencies per GHz, and then plotting the responses averaged over 1,000 successive equally-spaced frequencies. This was done to eliminate an artifact ripple in the simulated response, which resulted from the frequency sampling and limited integration time interval T.

The averaged response is in practice independent of T when T is longer than 10 ns or so, whereas for small T (∼0.1 ns) the PPR peak cannot be observed. This suggests that the main reason why PPR is not reported for FP lasers is that these lasers do not provide any mechanism to maintain the phase difference between the longitudinal modes. A mechanism for phase-coupling is associated with the presence of gratings so that distributed feedback (DFB) and DBR lasers can exhibit PPR. Supplementary, in DFB and DBR lasers the longitudinal mode spacing $\Delta\lambda$ can be influenced, which opens the possibility to obtain the PPR at 30–40 GHz even with relatively short L. Several PPR peaks (apart from the $\Delta m_{odd} \cdot \Delta\lambda \cdot c/\lambda^2$ series) might be induced in feedback lasers, particularly when multiple longitudinal cavities and/or detuned loading are employed, since several longitudinal mode spacings might be present in these lasers. However, the exploitation of these multiple resonances is hampered by various

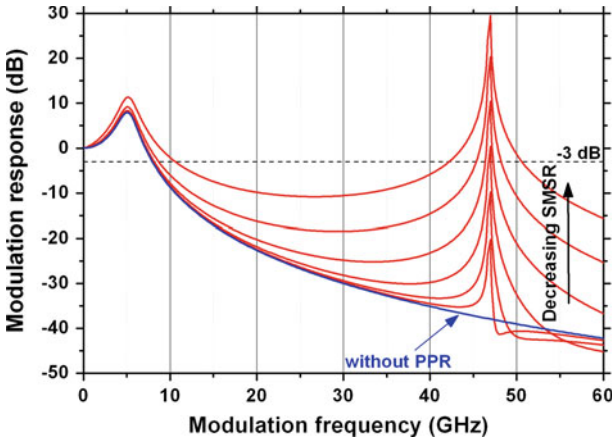

Fig. 1 Calculated $|H(\omega)|^2$ at 100 mA for a 1,000 μm long laser without including the PPR term and with the PPR term when the SMSR between the two successive dominant quasi-phase-locked longitudinal modes is 10, 20, 30, 40, 50 or 60 dB

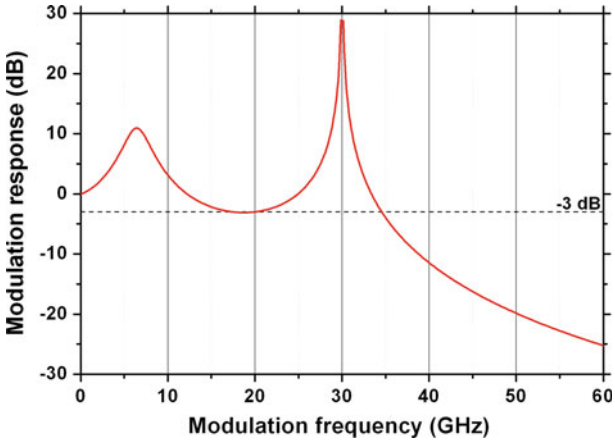

Fig. 2 Calculated $|H(\omega)|^2$ for a laser with detuned loading when the SMSR between the two dominant quasi-phase-locked longitudinal modes is 10 dB and the bias current is 120 mA

damping mechanisms when they occur at very high frequencies. Figure 2 presents the modulation response for a structure with 10 dB SMSR and 30 GHz mode spacing between the dominant modes. A high 3-dB modulation bandwidth is obtained when the device is biased above 120 mA.

6 Conclusions

We have shown that when the space and time dependence of the longitudinal confinement factor is included in the small-signal response analysis, the modulation transfer function has an extra term. When the laser has two dominant longitudinal modes that are phase-locked for long enough, this term introduces a PPR peak in the modulation response at a frequency

corresponding to the frequency separation between these modes. The PPR effect is stronger when the longitudinal modes are consecutive and phase-locked for longer, when their overlap integral is high (i.e. similar longitudinal field distribution envelopes) and their reciprocal SMSR is small. However, in order to increase the 3-dB modulation bandwidth by exploiting the PPR effect, a careful structure and operating regime analysis has to be carried out even when the PPR is available. Parasitic damping mechanisms and a flat modulation response between the CPR and PPR are critical issues in exploiting the PPR for enhanced modulation bandwidth.

Acknowledgments The work reported in this paper has been carried out within the EU FP7 project "Development of low-cost technologies for the fabrication of high-performance telecommunication lasers" (DeLight).

References

Bach, L., Kaiser, W., Reithmaier, J.P., Forchel, A., Gioannini, M., Feies, V., Montrosset, I.: 22-GHz modulation bandwidth of long cavity DBR laser by using a weakly laterally coupled grating fabricated by focused ion beam lithography. IEEE Photon. Technol. Lett. **16**, 18–20 (2004)

Coldren, L.A., Corzine, S.W.: Diode Lasers and Photonic Integrated Circuits. Wiley, New York (1995)

Feiste, U.: Optimization of modulation bandwidth of DBR lasers with detuned bragg reflectors. IEEE J. Quantum Electron. **34**, 2371–2379 (1998)

Gerschütz, F., Fischer, M., Koeth, J., Krestnikov, I., Kovsh, A., Schilling, C., Kaiser, W., Höfling, S., Forchel, A.: 1.3 μm quantum dot laser in coupled-cavity-injection-grating design with bandwidth of 20 GHz under direct modulation. Opt. Express **16**, 5596–5601 (2008)

Kaiser, W., Bach, L., Reuthmaier, J.P., Forchel, A.: High-speed coupled-cavity injection grating lasers with tailored modulation transfer functions. IEEE Photon. Technol. Lett. **16**, 1997–1999 (2004)

Kjebon, O., Schatz, R., Lourdudoss, S., Nilsson, S., Stålnacke, B., Bäckbom, L.: 30 GHz direct modulation bandwidth in detuned loaded InGaAsP DBR lasers at 1.55 μm. Electron. Lett. **33**, 488–489 (1997)

Morthier, G., Schatz, R., Kjebon, O.: Extended modulation bandwidth of DBR and external cavity lasers by utilizing a cavity resonance for equalization. IEEE J. Quantum Electron. **36**, 1468–1475 (2000)

Radziunas, M., Glitzky, A., Bandelow, U., Wolfrum, M., Troppenz, U., Kreissl, J., Rehbein, W.: Improving the modulation bandwidth in semiconductor lasers by passive feedback. IEEE J. Sel. Top. Quantum Electron. **13**, 136–142 (2007)